Published in final edited form as:
Biomacromolecules. 2008 April ; 9(4): 1200–1207. doi:10.1021/bm701201w.

Generating Elastic, Biodegradable Polyurethane/Poly(lactide-*co*-glycolide) Fibrous Sheets with Controlled Antibiotic Release via Two-Stream Electrospinning

Yi Hong[†,‡], **Kazuro Fujimoto**[†,‡], **Ryotaro Hashizume**[†,‡], **Jianjun Guan**[†,‡], **John J. Stankus**[†,§], **Kimimasa Tobita**[†,∥,⊥], and **William R. Wagner**[*,†,‡,§,∥]

[†]McGowan Institute for Regenerative Medicine, University of Pittsburgh, Pittsburgh, Pennsylvania 15219

[‡]Department of Surgery, University of Pittsburgh, Pittsburgh, Pennsylvania 15219

[§]Department of Chemical Engineering, University of Pittsburgh, Pittsburgh, Pennsylvania 15219

[∥]Department of Bioengineering, University of Pittsburgh, Pittsburgh, Pennsylvania 15219

[⊥]Department of Pediatrics, Children's Hospital of Pittsburgh, University of Pittsburgh, Pittsburgh, Pennsylvania 15219

Abstract

Damage control laparotomy is commonly applied to prevent compartment syndrome following trauma but is associated with new risks to the tissue, including infection. To address the need for biomaterials to improve abdominal laparotomy management, we fabricated an elastic, fibrous composite sheet with two distinct submicrometer fiber populations: biodegradable poly(ester urethane) urea (PEUU) and poly(lactide-*co*-glycolide) (PLGA), where the PLGA was loaded with the antibiotic tetracycline hydrochloride (PLGA-tet). A two-stream electrospinning setup was developed to create a uniform blend of PEUU and PLGA-tet fibers. Composite sheets were flexible with breaking strains exceeding 200%, tensile strengths of 5–7 MPa, and high suture retention capacity. The blending of PEUU fibers markedly reduced the shrinkage ratio observed for PLGA-tet sheets in buffer from 50% to 15%, while imparting elastomeric properties to the composites. Antibacterial activity was maintained for composite sheets following incubation in buffer for 7 days at 37 °C. In vivo studies demonstrated prevention of abscess formation in a contaminated rat abdominal wall model with the implanted material. These results demonstrate the benefits derivable from a two-stream electrospinning approach wherein mechanical and controlled-release properties are contributed by independent fiber populations and the applicability of this composite material to abdominal wall closure.

Introduction

Damage control laparotomy is a critical approach to decrease the metabolic insult associated with abdominal trauma. This approach includes an initial laparotomy (to control hemorrhage and contamination), intraabdominl packing, and temporary closure.[1,2] However, aggressive pre- and intraoperative resuscitation may result in massive edema of the bowel, compromising the surgeon's ability to complete primary abdominal closure. Primary closure of abdominal wall fascia under such circumstances would trigger the acute increase in intra-

*Corresponding author. Phone: +1-412-235-5138. Fax: +1-412-235-5110, wagnerwr@upmc.edu.

abdominal pressure, leading to abdominal compartment syndrome, which results in organ dysfunction and enhances risks of wound infection, fascial necrosis, and subsequent wound dehiscence.3 An obvious concern with an open abdominal field is infection.

Current materials that might be considered to reduce laparotomy-associated complications include those used for fascia reconstruction, materials used to create barrier films on tissue surfaces or for controlled-release applications, and biodegradable scaffolds used in tissue engineering applications. The first category would include nondegradable barrier fascia materials such as expanded poly(tetrafluoroethy1ene)4–6 and poly (propylene).7,8 While excellent results have been obtained with these materials in hernia management, their properties are nonideal for laparotomy in that they are nondegradable (and thus associated with a permanent foreign body response and acute infection risk), possess large pores with inadequate barrier properties (such as with polypropylene meshes,9) are mechanically stiff, and possess no intrinsic bioactivity. Hydrogel barriers, such those based on poly(ethylene glycol),10 chitosan,11,12 and other carbohydrate derivates,13,[14] can be biodegraded and may be engineered to incorporate bioactivity. Although these materials have been effectively used to prevent postsurgical abdominal adhesions, their applicability is limited in some settings due to their weak mechanical properties. In an application where a significant tensile load will be applied (e.g., with swelling tissue beds), or where suturability would be desirable, hydrogels generally are not appropriate. Materials derived from animal extracellular matrix, such as small intestinal submucosa[15] or bladder wall extracellular matrix,16 are attractive for fascia repair in that they possess intrinsic bioactivity and antimicrobial activity. Clinical and animal results obtained with these materials in a variety of placements have been attractive for their ultimate healing response.15,16 However, the disadvantage of these materials is that the initial mechanical properties, particularly elasticity, are limited. Additionally, we are not aware of any reports wherein loading of these materials with a specific exogenous bioactive compound or drug for controlled release has been achieved.

Our objective was to develop a material that would be amenable to the needs of temporary abdominal closure. Specifically we sought to develop a material that would possess elasticity, to allow for expansion and contraction of the material over the laparotomy wound bed as the exposed tissue swells and contracts. It was also a requirement that the material have the capacity for acute delivery of antibiotic agents, to reduce the infection risk in the period when the field remains open. Other desired features of the material included biodegradability, the ability to provide a mechanical barrier to contamination, strength without thickness, and suturability. To accomplish these design objectives, we developed a composite material by a modified two-stream electrospinning process wherein submicrometer scale fibers of a biodegradable elastomer, poly(ester urethane) urea (PEUU), [17] were blended on a microscale with fibers of poly(lactic-*co*-glycolic acid) (PLGA). The PEUU fibers served to provide elasticity to the resulting fibrous sheets while the PLGA fibers served as depots for the controlled release of a model antibiotic, tetracycline hydrochloride (tet). We report here on the generation and characterization of these fibrous sheets in terms of their morphology, mechanical properties, tetrelease kinetics, and antimicrobial activity. Several tet loading concentrations were examined, and PLGA fibrous sheets variably loaded with tet served as control groups. To demonstrate material functionality in vivo, acute placement of the developed material in an infected abdominal wall rat model was investigated.

Materials and Methods

Materials

Poly(lactide-*co*-glycolide) (PLGA, 50/50, weight average molecular weight = 40000–75000, Sigma), tet (Sigma, United States), stannous octoate (Sigma), 1,1,1,3,3,3-hexafluoro-2-propanol (HFIP, Oakwood Products, United States), and fluorescein isothiocyanate isomer I (FITC, Fluka, Switzerland) were used as received. Polycaprolactone diol (number average molecular weight = 2000, Sigma) was dried under vacuum for 48 h to remove residual water. 1,4- Diisocyanatobutane (Fluka) and putrescine (Fluka) were distilled under vacuum. Dimethyl sulfoxide (DMSO, Sigma) was dried over 4 Å molecular sieves. PEUU was synthesized as previously reported.[17]

Sheet Fabrication from PLGA–tet and PEUU via Single Stream Electrospinning

PLGA (15%, w/v) in HFIP was blended with tet at 1, 5, 10, and 20 wt % tet to PLGA. The mixed solution was fed at 0.5 mL/h by syringe pump (Harvard Apparatus, United States) into a steel capillary (1.2 mm i.d.) that was suspended 13 cm over a stainless steel mandrel (19 mm diameter) rotating at 250 rpm. The mandrel was attached to an *x*– *y* stage (Velmex, United States) that reciprocally translated in the direction of the mandrel axis at a speed of 8 cm/s and with an amplitude of 8 cm. Two high-voltage generators (Gamma High Voltage Research, United States) were employed to charge the steel capillary to 20 kV and the mandrel to −10 kV, respectively. Electrospinning of the polymer solution proceeded for approximately 4 h, after which the deposited PLGA-tet fibrous sheets were removed from the mandrel using a blade to cut along the length of the mandrel. The sheets were dried in a vacuum oven at room temperature overnight. Material samples were cut for testing and kept in a dark environment until use to preserve bioactivity. PLGA-tet1, −5, −10, and −20, refer to PLGA fibrous sheets loaded with 1, 5, 10, and 20 wt % tet, respectively.

PEUU (12%, w/v) in HFIP was fed at 1.5 mL/h by syringe pump into a steel capillary (1.2 mm i.d.) that was suspended 18 cm over a stainless steel mandrel (11 cm diameter) rotating at 250 rpm. As above, the mandrel was attached to an *x*– *y* stage that reciprocally translated in the direction of the mandrel axis at a speed of 8 cm/s but with an amplitude of 6 cm. The voltages utilized for the capillary and mandrel were 12 and −10 kV, respectively, and the process for sheet removal was as described for PLGA-tet sheets.

Fabrication of PEUU/PLGA-tet Fibrous Sheets by Two-Stream Electrospinning

Two-stream electrospinning was achieved by the simultaneous electrospinning of PLGA-tet and PEUU from two perpendicular capillaries as shown in Figure 1. PLGA (15% w/v) in HFIP was blended with tet (1, 5, 10, and 20 wt % of PLGA), and the mixed solution was fed at 0.5 mL/h by syringe pump into a 1.2 mm id steel capillary positioned 13 cm over a 11 cm diameter stainless steel mandrel rotating at 250 rpm. PEUU (12%, w/v) in HFIP was simultaneously fed at 1.5 mL/h by syringe pump into a separate but identical steel capillary that was positioned perpendicular to the first capillary in the plane of mandrel rotation and 18 cm from the mandrel. The mandrel reciprocally translated at a 6 cm amplitude and a speed of 8 cm/s. Three high-voltage generators were employed to charge the steel capillary loaded with PLGA/tet solution at 20 kV, the steel capillary loaded with PEUU at 12 kV and the mandrel at −10 kV. After electrospinning for approximately 4 h, the sheet was removed, dried, and sectioned as described above. The fibrous sheets were referred to as PEUU/PLGA-tet1, −5, −10, or −20 based on the tet content.

Sheet Characterization

The morphology of electrospun sheets was observed under field emission scanning electron microscopy (FE-SEM, JEOL JSM6330F, Japan) after drying and gold sputter coating. Fiber

diameter distributions were measured by ImageJ software (NIH, United States). Fluorescent microscopy (Nikon E800, Japan) was used to visualize the distinct fiber types within sheets derived from two-stream processing. To accomplish this, sheets comprised only of PLGA (which was autofluorescent) or PEUU (mixed with FITC prior to electrospinning) were observed at emission wavelengths of 543 and 488 nm, respectively, to optimize the exposure time. Sheets of PEUU/PLGA were imaged at both 543 and 488 nm and the images were merged to visualize both fiber types.

The mass fraction of PEUU in composite sheets was measured by immersing the samples in acetone to remove PLGA fibers. Acetone was replaced every 30 min, five times, after which samples were dried in a vacuum oven at 37 °C for 24 h. The dried sample was weighed (W_1) and the PEUU content was calculated as $W_1/W_0 \times 100\%$ where W_0 represented the sample weight prior to acetone treatment. Four samples were tested at each condition studied.

Mechanical properties of the fibrous sheets cut into strips (2 × 15 mm) were measured on an MTS Tytron 250 MicroForce Testing Workstation (United States) at a 10 mm/min crosshead speed, according to ASTM D638-98. At least five samples were tested for each sheet composition. Instant strain recovery was tested under the same conditions. The samples were marked at their distal ends, stretched to 50% strain and held for 1 min, and then released. The original length (L_0) and the length immediately after releasing the strain (L_1) were measured by caliper. Instant strain recovery was calculated as $(1 - (L_1 - L_0)/L_0) \times 100\%$. Suture retention strength was tested with a BIOSYN UM-214 4-0 suture (Syneture, USA) under the same conditions. A longitudinally cut strip from a Gore-Tex vascular graft (W. L. Gore & Associate, USA; graft internal diameter, 6 mm) was used for control purposes. A single suture loop was created 5 mm from the short edge and fixed on the upper clamp. Suture retention strength was calculated as suture load/(suture diameter × sample thickness) at the point of tearing.

The shrinkage ratio of the fibrous sheets in aqueous buffer was obtained by placing 10 mm diameter sheets made using a biopsy punch into phosphate buffered saline (PBS) at 37 °C. After 24 h the sheet diameter (D_1) was measured in millimeters and the shrinkage ratio was calculated as $(10 - D_1)/10 \times 100\%$. Four samples were tested for each sheet composition.

Temporal Release of tet

Temporal release of tet from PLGA-tet and PEUU/PLGA-tet fibrous sheets was measured from 10 mm diameter disks obtained using a biopsy punch. After being weighed, each sample was immersed in 5 mL of PBS at 37 °C in a dark environment. The buffer volumes and collection times utilized ensured that sink conditions were maintained for tet release. At each time point, all 5 mL of the buffer was collected and replaced with 5 mL of fresh PBS. The collected buffer samples were stored at −20 °C. After collection of the last buffer sample (at 2 weeks), the collected samples were thawed and UV absorbance was measured at 360 nm (Perkin-Elmer UV/vis Lambda 40, United States). A standard curve was obtained by measuring different concentrations of tet/PBS solution on a UV–vis spectrometer at 360 nm. Four disks were tested temporally for each composition studied.

Bacterial Inhibition Activity

Disks (6 mm diameter, 0.2 mm thick) were punched from PEUU/PLGA-tet sheets and immersed in PBS at 37 °C for 0, 3, and 7 days, respectively, after which the samples were washed with fresh PBS three times to remove any residual solution. *Escherichia coli* K12 (*E. coli*, ATCC 12345, The American type Culture Collection, USA; 100 μL at a concentration of 10^6/mL) were spread uniformly over the surface of agar gel in 11 cm Petri dishes, and PEUU/PLGA-tet disks, with or without previous PBS incubation, were placed

on this surface. All dishes were inverted and placed in a 37 °C incubator. After 24 h, the diameter of antibacterial activity was measured by a caliper. A PEUU fibrous sheet was used as a control. Four disks were tested for each composition studied.

In Vivo Assessment

Adult female Lewis rats (Harlan Sprague-Dawley, Indianapolis, IN) weighing (200–250 g), were used. The research protocol followed the National Institutes of Health guidelines for animal care and was approved by the University of Pittsburgh's Institutional Animal Care and Use Committee and Children's Hospital of Pittsburgh Animal Research Care Committee. To implant fibrous sheets into a contaminated abdominal wall model, first the abdominal cavity was exposed by creating a 3 cm long, full-thickness incision approximately 2 cm inferior to the xiphoid process. The peritoneal cavity was lavaged with sterile saline, and injected with rat stool slurry (0.25 mL).[18] The slurry was previously prepared by homogenizing 1 g of rat stool in 20 mL of normal saline. Using 7-0 polypropylene with over-and-over sutures, a 2.5 × 0.5 cm piece of either PEUU or PEUU/PLGA-tet20 sheet was interposed within the incision space (PEUU $n = 5$, PEUU/PLGA-tet20 $n = 5$). The skin and subcutaneous tissue were closed with 4-0 Vicryl interrupted suture. All animals were sacrificed after a 1 week implantation period. The implant site was quantitatively assessed for wound dehiscence with digital image processing of images of the suture line. Following opening of the sutures, the implant site above and below the implanted sheets was qualitatively scored for the extent of abscess formation.

Statistical Analysis

Results are displayed as the mean ± standard deviation. One-way ANOVA was utilized to evaluate the shrinkage ratio, mechanical properties, and antibacterial activity using the Neuman-Keuls test for post hoc assessment of the differences between specific samples. Significance was considered to exist if $p < 0.05$.

Results

PLGA-tet Sheets and PEUU Sheets via Single-Stream Electrospinning

Randomly oriented, smooth, and continuous submicrometer-scale fibers were obtainable for PLGA-tet with 1 to 20 wt % antibiotic. A typical electron micrograph of a fibrous sheet surface is seen in Figure 2A for PLGA-tet20. The fiber diameters for the PLGA-tet materials were 144 ± 45 nm for PLGA-tet1, 102 ± 27 nm for PLGA-tet5, 116 ± 40 nm for PLGA-tet10, and 198 ± 57 nm for PLGA-tet20. No obvious trend was present in morphology as tet content was varied. For PEUU fibrous sheets, which were processed under slightly different conditions, larger diameter fibers (390 ± 120 nm) resulted, as seen in Figure 2B.

PEUU/PLGA-tet Sheets via Two-Stream Electrospinning

As shown in Figure 3, fluorescent imaging demonstrated uniform blending between PEUU and PLGA fibers. Scanning electron micrographs also showed continuous fiber morphologies of these composite sheets at all tet concentrations (1, 5, 10, and 20 wt % of PLGA fraction) (Figure 2C–F). On the basis of the appearance of PLGA-tet and PEUU fibrous sheets individually, the presence in the composite sheets of distinct populations of larger and smaller diameter fibers was attributed to PEUU and PLGA-tet streams, respectively. Examination of the fiber diameter distributions of PEUU/PLGA-tet20, PEUU, and PLGA-tet20 fibrous sheets in Figure 4 supports this interpretation with the most frequent fiber diameters in the single-component sheets corresponding to the peaks of the bimodal fiber diameter frequency distribution in the composite sheet. To further quantify the PEUU content in the composite sheets, PLGA-tet fibers were removed by acetone washing.

As shown in Table 1, the PEUU content in composite sheets ranged from 57 to 69 wt %, which was generally lower than the theoretical value expected based on polymer solution mass flow rates during processing. The antibiotic content in the composite sheets was calculated for the composite fibers based upon the measured PLGA mass fraction in the composite sheets.

Mechanical Properties

The mechanical properties of the fibrous sheets are summarized in Table 2. The initial modulus ($p < 0.05$) and tensile strength ($p < 0.05$) of PLGA-tet sheets decreased with increasing tet content, and a trend toward lower breaking strain with increasing tet content was observed. PEUU alone had a tensile strength of 12 ± 1 MPa and breaking strain of 191 ± 15%. The initial moduli of PEUU/PLGA-tet sheets ranged from 8 to 11 MPa and were significantly lower than those for the corresponding tet content PLGA-tet sheets (14–55 MPa; $p < 0.05$) and higher than that for PEUU alone (6 MPa; $p < 0.05$). Tensile strengths of the composite sheets were 5–7 MPa and were significantly higher than the corresponding PLGA-tet sheets ($p < 0.05$) with the exception of the 1 wt % tet content sheets which were similar. All composite sheet tensile strengths were lower than the PEUU sheet ($p < 0.05$). The breaking strains of the PEUU/PLGA-tet composite sheets were around 200%, which was similar to that found for the PEUU sheet and significantly higher than that of PLGA-tet sheets, which ranged from 21 to 61%. Instant strain recovery for PEUU sheets (99%) was significantly higher than that for composite sheets ($p < 0.05$). Instant strain recovery of PEUU/PLG-Atet5, −10, and −20 sheets was approximately 87%, which was significantly lower than PEUU/PLGA-tet1 (91%, $p < 0.05$). Suture retention strengths for PEUU/PLGA-tet sheets ranged from 30 to 44 N/mm^2, which was significantly lower than for the PEUU sheet (71 N/mm^2) but significantly higher than that for the Gore-Tex vascular graft control (23 N/mm^2).

Sheet Contraction

After PLGA-tet sheets were immersed in PBS at 37 °C for 24 h, substantial shrinkage was observed (Figure 5A,B). However, for PEUU and PEUU/PLGA-tet sheets the shrinkage was markedly less and not apparent upon gross inspection (Figure 5A,B). As shown in Figure 5C, PLGA-tet sheets had shrinkage ratios around 45%, with PLGA-tet20 experiencing significantly greater shrinkage of 52% ($p < 0.05$). PEUU experienced 7% shrinkage and PEUU/PLGA-tet sheets contracted by approximately 15%. Figure 6 illustrates the surface morphologies of PLGA-tet, PEUU/PLGA-tet, and PEUU sheets after the 24 h of PBS incubation. PLGA-tet sheet surfaces lost their original fibrous morphologies whereas PEUU/PLGA-tet and PEUU sheets remained fibrous. Of note the smaller, putative PLGA fibers in the PEUU/PLGA-tet composite sheets were no longer apparent, although the PLGA fibers may have swelled to approximate PEUU fiber diameters or melded onto PEUU fibers. PLGA fibrous sheets without tet incorporation demonstrated the same loss of fibrous morphology after 24 h of PBS incubation (data not shown).

tet Release

Tetracycline hydrochloride periodic release profiles from PLGA-tet and PEUU/PLGA-tet sheets are shown in logarithmic time scale in Figure 7. By 3 h the burst release from PLGA-tet sheets (Figure 7A) is finished and only low-level release occurs, which becomes apparent as the collection time periods are increasingly lengthened. In contrast, for PEUU/PLGA-tet sheets the relative burst period continues for approximately 96 h. In terms of % tet released, PLGA-tet scaffolds had 55–90% tet remaining after 14 days whereas PEUU/PLGA-tet had 0–65% remaining after this period. Of note, the PEUU/PLGA-tet scaffolds have approximately 30–40% of the tet content of the corresponding PLGA-tet scaffolds due to the 60–70% mass fraction of PEUU fibers (Table 1).

Bacterial Inhibition by tet-Loaded Sheets

The ability of PEUU/PLGA-tet sheets to kill *E. coli* bacteria and inhibit growth for 24 h is shown in Figure 8 for sheets following 0, 3, and 7 days of incubation in PBS. PEUU fibrous sheets served as controls. All of the PEUU/PLGA-tet sheets examined at all of the time points demonstrated antibacterial diameters that were significantly higher than the PEUU control. Original samples (0 days) had antibacterial diameters ranging from 13 to 27 mm, increasing with the loaded tet content. After 3 days of incubation the PEUU/PLGA-tet1 and PEUU/PLGA-tet5 sheets had markedly smaller antibacterial zones than the PEUU/PLGA-tet10 and PEUU/PLGA-tet20 sheets. At 7 days the differences between the composites with varying tet content were not as pronounced, although the PEUU/PLGA-tet10 composite sheet was found to have a significantly larger antibacterial diameter than the other three composites.

In Vivo Assessment

Both types of implanted sheets, PEUU (control) and PEUU/PLGA-tet20, were found to handle well. surgically and were easily sutured onto the tissue. There were no postoperative deaths in either surgical group. At the time of explantation, before opening the suture line, substantial wound dehiscence was apparent in three of five animals implanted with PEUU sheets, whereas only one of five PEUU/PLGA-tet20 rats had very minor dehiscence (Figure 9A,B). This was quantified by image processing and reported in Table 3. After the implantation site was opened, abscess formation above the implanted material was observed only in PEUU sheet implants, none was found above PEUU/PLGA-tet20 sheets. Beneath the material, abscesses were found in all PEUU sheet implants at levels scored to be moderate to severe, whereas under PEUU/PLGA-tet20 sheets no abscesses were found (Figure 9C,D, Table 3). For both material types, tissue adhesions could be detached with no bleeding. No significant material shrinkage was observed for either material at the time of explantation, with both materials being greater than 95% of their original implanted dimensions.

Discussion

Previous Electrospinning Work

The use of electrospinning for biomaterials processing has generated a great deal of excitement over the past several years in the research community and offers a relatively straightforward means to generate materials comprised of nano- to microscale fibers. When applying this technique to PEUU, we have previously reported on the generation of strong and elastic matrices[19,20] that would meet our desire in the current work to generate a material capable of distending with tissue swelling and contracting during healing as well. PEUU has also recently been shown to offer attractive controlled-release properties with basic fibroblast growth factor21 and others have shown controlled release from a variety of electrospun polymers,[22–30] so the concept of incorporating an antibiotic into electrospun PEUU for abdominal wall closure was initially investigated. However, our early results with electrospun PEUU-tet showed a large burst release of tet over a 24 h period with no significant further release (data not presented). This motivated us to explore the generation of a composite fibrous material where PEUU would contribute mechanical properties while a second polymer would be employed as a reservoir for controlled release.

Previous reports in the literature have employed multiple feed streams in electrospinning to introduce structural and property complexity in the deposited materials and to prepare polymeric sheets rapidly and uniformly when each of the multiple streams have contained the same material.[31–33] Coaxial tube electrospinning has been employed to create a core–shell fiber with drug or protein loading in one of the two components27,28 and multijet electrospinning has been reported where composite fibrous sheets resulted with distinct fiber

compositions.[34–38] With respect to the latter, two-stream electrospinning has been reported by Kidoaki et al. where a composite of segmented (nondegradable) polyurethane fibers and poly(ethylene oxide) fibers were generated from side-by-side streams electrospun through a hole onto a rotating and reciprocating mandrel.[35] PLGA and a chitosan/poly(vinyl alcohol) solution in one instance and poly(caprolactone) and poly(vinyl alcohol) in another case were utilized to generate composite sheets fabricated by two side-by-side streams with target movement to minimize stream repulsion effects.[37,38] In those reports the additions of chitosan/poly(vinyl alchohol) or poly(vinyl alcohol) fibers were employed to increase the hydrophilicity of PLGA fibrous meshes and to positively influence cellular growth. Although multijet electrospinning has been used previously to generate composite matrices with distinct hydrophilic characteristics, there are no reports to our knowledge where a second stream has been utilized in processing to blend in fibers for the purpose of imparting controlled release of a drug or growth factor.

When side-by-side capillaries are used for electrospinning, the depositing fibers from different capillaries repel each other due to their similar charge and make achieving a uniformly blended material a challenge.[32,35] Our preliminary experience confirmed that stream repulsion effects introduced axial variations in materials deposited onto a rotating mandrel, despite the reduction of this effect with cyclic translation of the mandrel (data not shown). For this reason we employed two capillaries positioned on the same plane but offset 90° from one another to reduce the repulsion effects and to obtain a uniformly deposited composite. In development of this technique, it was found that increasing the viscosity of the polymer solution loaded in the side capillary by increasing the polymer concentration over what might be optimal for a vertically oriented capillary was necessary to provide effective polymer spinning and deposition. The discrepancies in the theoretical versus measured PEUU content of the composite fibrous sheets (Table 1) indicate that the deposition process is still likely subject to variation from absolutely even and complete deposition of the two fiber types. The discrepancies found in these data could be attributed to variations in fiber deposition (e.g., errant fibers not depositing on the mandrel), temporal variation in relative polymer mass deposited, or local inhomogeneities in the distribution of fiber types deposited. Visual inspection with labeled fibers suggested that the latter explanation did not appear to be likely.

Addressing Mechanical Limitations of PLGA Alone (Shrinkage, Stiffness)

The mechanical properties of the PEUU/PLGA-tet composite were found to lie between those of PEUU and PLGA-tet, respectively, as might be expected. In previous reports of two-stream processing with PLGA-chitosan/poly(vinyl alcohol) and poly(caprolactone)/poly(vinyl alcohol) a similar moderation of mechanical properties between the two components was reported.[36,37] In the PEUU/PLGA-tet composite the presence of the PLGA fibers likely acts to reduce the density of PEUU-PEUU fiber interactions. Tensile loading would act to initially load the PLGA fibers preferentially (resulting in a higher initial modulus), but at the 100% strain point when a meaningful number of PLGA fibers had broken, the load would be taken by the PEUU fibers. Since the PEUU fibers in the composite are less self-connected, this would lead to a lower 100% modulus and a greater breaking strain. We generally observed these trends, as seen in Table 2.

A major limitation that was found in examining electrospun PLGA-tet sheets, in addition to the inherent stiffness of this material, was the substantial shrinkage that occurred after immersion in PBS at 37 °C for 24 h. This effect has been previously observed with PLGA electrospun fibrous sheets and has been attributed to fiber swelling (in diameter) and shortening (in length) in PBS at 37 °C.[29,39,40] The higher shrinkage ratio observed in the PLGA-tet20 might be attributed to the lower mechanical properties found with the increased tet content in the PLGA fibers and to the higher hydrophilicity one would expect with

increasing tet, which would contribute to the fiber swelling and sheet shrinkage. Such pronounced shrinkage behavior would be undesirable for abdominal wall patch application in that it would contribute to dehiscence of the material from the wound border and compromise the barrier effect.29,[30] The shrinkage ratio of the PLGA-tet sheet was improved from ~50% to ~15% by forming composites with PEUU fibers, which independently showed low shrinkage ratios of approximately 5%. This benefit from the PEUU component was in addition to the elasticity observed in the sheets upon introduction of this elastomer, which would provide for the desired expansion and contraction ability that we sought to achieve for the abdominal wall closure application.

Addressing Limitations of PEUU tet Release and PLGA tet Release

Verreck et al. have reported on controlled release over a 24 h period from nondegradable electrospun polyurethane matrices. Itraconazole-loaded fibers provided a 24 h linear release at pH = 4 and 37 °C, while ketanserin-loaded fibers experienced a 4 h burst release and then linear release under the same conditions.[23] In both cases the release was effectively complete at 24 h. Our experience with tet-loaded electrospun PEUU was similar in that near complete release occurred over a 24 h period with an initial burst effect. As mentioned previously, this provided the impetus to devise a composite scaffold where we mixed PLGA (50/50) fibers as antibiotic carriers with PEUU fibers.

Previous investigators have evaluated electrospun PLGA for controlled release and demonstrated attractive features. PLGA (75/25) fibers loaded with 5% cefoxitin sodium experienced slow release for 168 h after 1 h of burst release.[25] Paclitaxel-loaded PLGA (50/50) fibers electrospun in dimethylene chloride provided 2 months of sustained release in PBS after a 24 h burst release.24 We found that tet-loaded PLGA fibrous sheets experienced a 1 h burst release, followed by a low release rate that then increased significantly after approximately 1 week. The burst effect was attributed to the large fiber surface area and highly soluble surface-segregated tet.23 The low release period may have been due to the observed swelling in the PLGA fibers to form what appeared to be a dense shell that provided a barrier to further tet release. After 1 week, PLGA degradation may have led to an increased tet release from the polymer bulk phase. The composite PEUU/PLGA-tet sheets experienced 96 h of sustained release after a 1 h burst and then release at a lower rate until 2 weeks. The composite structure formed between the two fiber types might explain the differences observed. The PEUU fibers appeared to largely maintain their original structure and thus prevented the shell formation observed with PLGA fibers alone. The swelled PLGA fibers in the case of the composite sheets likely swelled to approximate PEUU fiber diameters and were kept separated by the PEUU fibers or the PLGA fibers melded and associated with the PEUU fibers, as is seen when comparing images from Figure 2 and Figure 6.

Initial in Vivo Assessment and Study Limitations

The maintenance of antibacterial activity by the composite sheets even after incubation for 7 days in buffer and rinsing was encouraging. The antibacterial activity was modest for the lower tet concentrations (tet1 and tet5), likely due to the reduced amounts of tet remaining in the PLGA fibers, but extended release beyond 1 week may not be required in many applications. This in vitro result appeared to translate to the in vivo setting where PEUU/PLGA-tet20 sheets were shown to abrogate abscess formation and wound dehiscence in a rat abdominal model with fecal contamination. A limitation of this animal model is the possibility that early burst release of tet was responsible for bacterial killing and extended release periods may not have been necessary. A second-level in vivo study with ongoing bacterial contamination could potentially address this concern, although for the clinical setting the current model has direct value. Once sutured in place, one might expect new

contamination from above the material, but below the material this would be substantially less likely. Additionally, in a controlled clinical setting initial wound debridement could be maintained to reduce the likelihood of bacterial entrance from the wound site. Clearly more in vivo work will be necessary to characterize the local tissue responses to the composite materials for longer implantation periods, in larger animal models, and with different antibiotics that may have greater relevance to clinical application.

The PEUU/PLGA-tet sheets might ultimately be applicable in a variety of settings where there is direct exposure to the external environment or where there is the potential, either initially or with time, to close the open wound field. PEUU/PLGA sheets loaded with other components might also find application in other clinical areas such as in the repair of fasciotomies in the extremities and the prevention of postsurgical adhesions.[29,30]

Conclusions

A method has been developed for the creation of an elastomeric, fibrous sheet capable of sustained antibacterial activity in vitro. In development of this material, a novel approach to two-stream electrospinning was pursued wherein one component stream provided for antibiotic release while the other provided mechanical properties deemed essential for the desired application. This material may ultimately find applicability in the treatment of temporary abdominal wall closure.

Acknowledgments

We acknowledge the financial support from the US Army/DAMD #17-02-1-0717A and NIH #HL069368. We also are grateful for the help of Dr. Richard Koepsel with antibacterial testing.

References and Notes

1. Neuhaus SJ, Bessell JR. ANZ J. Surg 2004;74:18–22. [PubMed: 14725699]
2. Lee JC, Peitzman AB. Curr. Opin. Crit. Care 2006;12:346–350. [PubMed: 16810046]
3. Fabian TC. Surg. Clin. North Am 2007;87:73–93. [PubMed: 17127124]
4. Diaz JJ, Gray BW, Dobson JM, Grogan EL, May AK, Miller R, Guy J, O'Neill P, Morris JA. Am. Surg 2004;70:396–401. [PubMed: 15156946]
5. Vertrees A, Kellicut D, Ottman S, Peoples G, Shriver C. J. Am. Coll. Surg 2006;202:762–772. [PubMed: 16648016]
6. Dumanian GA. Plast. Reconstr. Surg 2006;117:312–313. [PubMed: 16404285]
7. Hasegawa S, Yoshikawa T, Yamamoto Y, Ishiwa N, Morinaga S, Noguchi Y, Ito H, Wada N, Inui K, Imada T, Rino Y, Takanashi Y. Surg. Today 2006;36:1058–1062. [PubMed: 17123133]
8. Burger JWA, Halm JA, Wijsmuller AR, ten Raa S, Jeekel J. Surg. Endosc 2006;20:1320–1325. [PubMed: 16865616]
9. Belĺ, on JM, Contreras LA, Buján J, Palomares D, Carrera-San Martín A. Biomaterials 1998;19:669–675. [PubMed: 9663739]
10. Sawhney AS, Pathak CP, Vanrensburg JJ, Dunn RC, Hubbell JA. J. Biomed. Mater. Res 1994;28:831–838. [PubMed: 8083251]
11. Yeo Y, Burdick JA, Highley CB, Marini R, Langer R, Kohane DS. J. Biomed. Mater. Res., Part A 2006;78A:668–675.
12. Zhou J, Elson C, Lee TDG. Surgery 2004;135:307–312. [PubMed: 14976481]
13. Liu WG, Zhang BQ, Lu WW, Li XW, Zhu DW, Yao KD, Wang Q, Zhao CR, Wang CD. Biomaterials 2004;25:3005–3012. [PubMed: 14967533]
14. Yeo Y, Highley CB, Bellas E, Ito T, Marini R, Langer R, Kohane DS. Biomaterials 2006;27:4698–4705. [PubMed: 16750564]
15. Dedecker F, Grynberg M, Staerman F. Prog. Urol 2005;15:405–410. [PubMed: 16097143]

16. Brown B, Lindberg K, Reing J, Stolz DB, Badylak SF. Tissue Eng 2006;12:519–526. [PubMed: 16579685]
17. Guan JJ, Sacks MS, Beckman EJ, Wagner WR. J. Biomed. Mater. Res 2002;61:493–503. [PubMed: 12115475]
18. An G, Walter RJ, Nagy K. J. Trauma 2004;56:1266–1275. [PubMed: 15211136]
19. Stankus JJ, Guan JJ, Wagner WR. J. Biomed. Mater. Res., Part A 2004;70A:603–614.
20. Stankus JJ, Guan JJ, Fujimoto K, Wagner WR. Biomaterials 2006;27:735–744. [PubMed: 16095685]
21. Guan JJ, Stankus JJ, Wagner WR. J. Controlled Release 2007;120:70–78.
22. Kenawy ER, Bowlin GL, Mansfield K, Layman J, Simpson DG, Sanders EH, Wnek GE. J. Controlled Release 2002;81:57–64.
23. Verreck G, Chun I, Rosenblatt J, Peeters J, Dijck AV, Mensch J, Noppe M, Brewster ME. J. Controlled Release 2003;92:349–360.
24. Xie JW, Wang CH. Pharm. Res 2006;23:1817–1826. [PubMed: 16841195]
25. Kim K, Luu YK, Chang C, Fang DF, Hsiao BS, Chu B, Hadjiargyrou M. J. Controlled Release 2004;98:47–56.
26. Cui WG, Li XH, Zhu XL, Yu G, Zhou SB, Weng J. Biomacromolecules 2006;7:1623–1629. [PubMed: 16677047]
27. Zhang YZ, Wang X, Feng Y, Li J, Lim CT, Ramakrishna S. Biomacromolecules 2006;7:1049–1057. [PubMed: 16602720]
28. Huang ZM, He CL, Yang AZ, Zhang YZ, Han XJ, Yin JL, Wu QS. J. Biomed. Mater. Res., Part A 2006;77A:169–179.
29. Zong XH, Li S, Garlick B, Kim K, Fang DF, Chiu J, Zimmerman T, Brathwaite C, Hsiao BS, Chu B. Ann. Surg 2004;240:910–915. [PubMed: 15492575]
30. Bölgen N, Vargel İ, Korkusuz P, Menceloğlu YZ, Pişkin E. J. Biomed. Mater. Res., Part B 2007;81B:530–543.
31. Teo WE, Ramakrishna S. Nanotechnology 2006;17:R89–R106. [PubMed: 19661572]
32. Theron SA, Yarin AL, Zussman E, Kroll E. Polymer 2005;46:2889–2899.
33. Kim G, Cho YS, Kim WD. Eur. Polym. J 2006;42:2031–2038.
34. Madhugiri S, Dalton A, Gutierrez J, Ferraris JP, Balkus KJ. J. Am. Chem. Soc 2003;25:14531–14538. [PubMed: 14624602]
35. Kidoaki S, Kwon IK, Matsuda T. Biomaterials 2005;26:37–46. [PubMed: 15193879]
36. Kim CH, Khil KS, Kim HY, Lee HU, Jahng KY. J. Biomed. Mater. Res., Part B 2006;78B:283–290.
37. Duan B, Yuan XY, Zhu Y, Zhang YY, Li XL, Zhang Y, Yao KD. Eur. Polym. J 2006;42:2013–2022.
38. Ding B, Kimura E, Sato T, Fujita S, Shiratori S. Polymer 2004;45:1895–1902.
39. Zong XH, Ran SF, Kim KS, Fang DF, Hsiao BS, Chu B. Biomacromolecules 2003;4:416–423. [PubMed: 12625740]
40. Li WJ, Cooper JA, Mauck RL, Tuan RS. Acta Biomater 2006;2:377–385. [PubMed: 16765878]

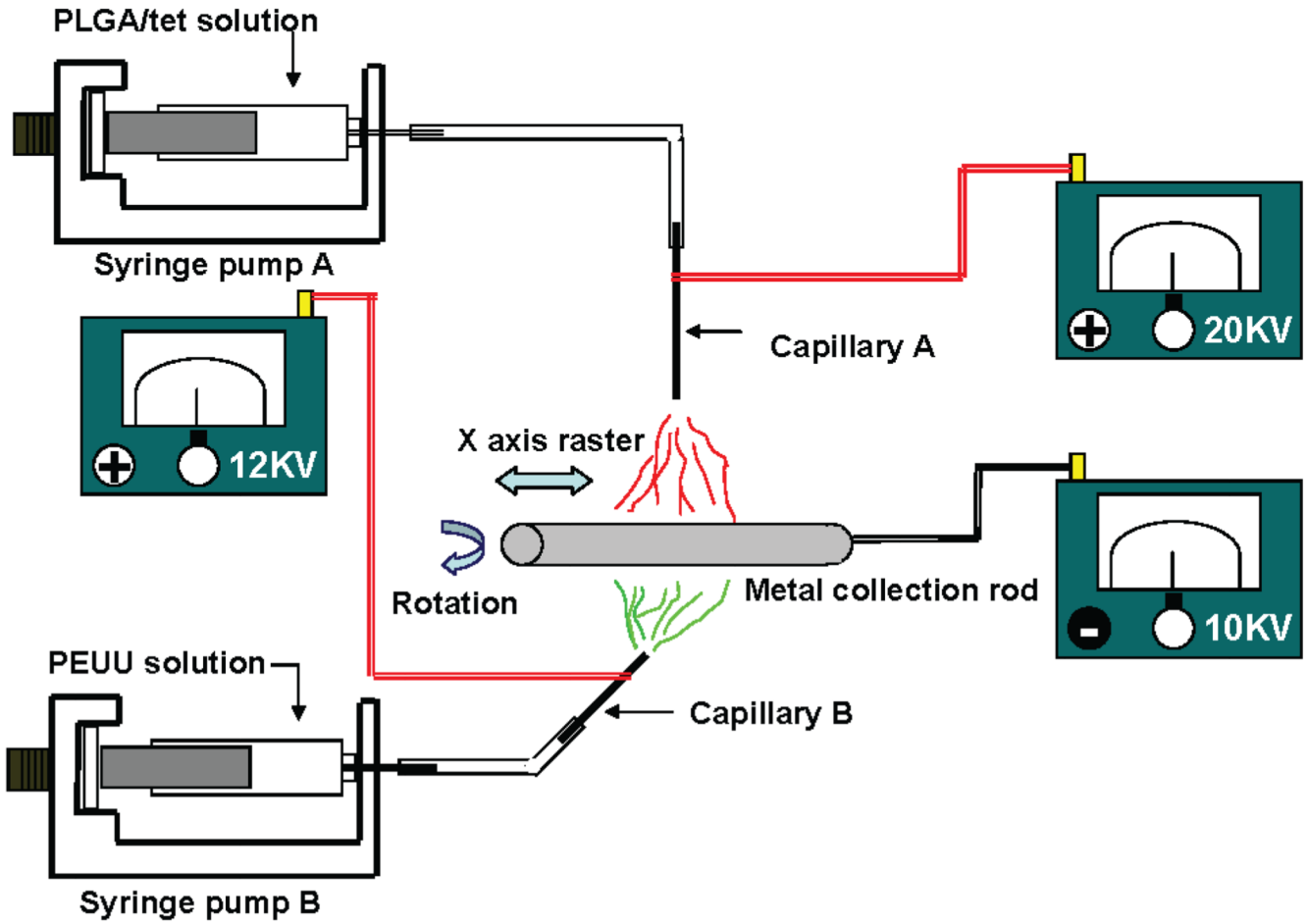

Figure 1.
Two-stream electrospinning setup consisted of two syringe pumps to feed polymer solutions along with a combination of three high-voltage generators and a rotating metal rod that reciprocated on an *x*–*y* stage. The two capillaries were located perpendicular to each other.

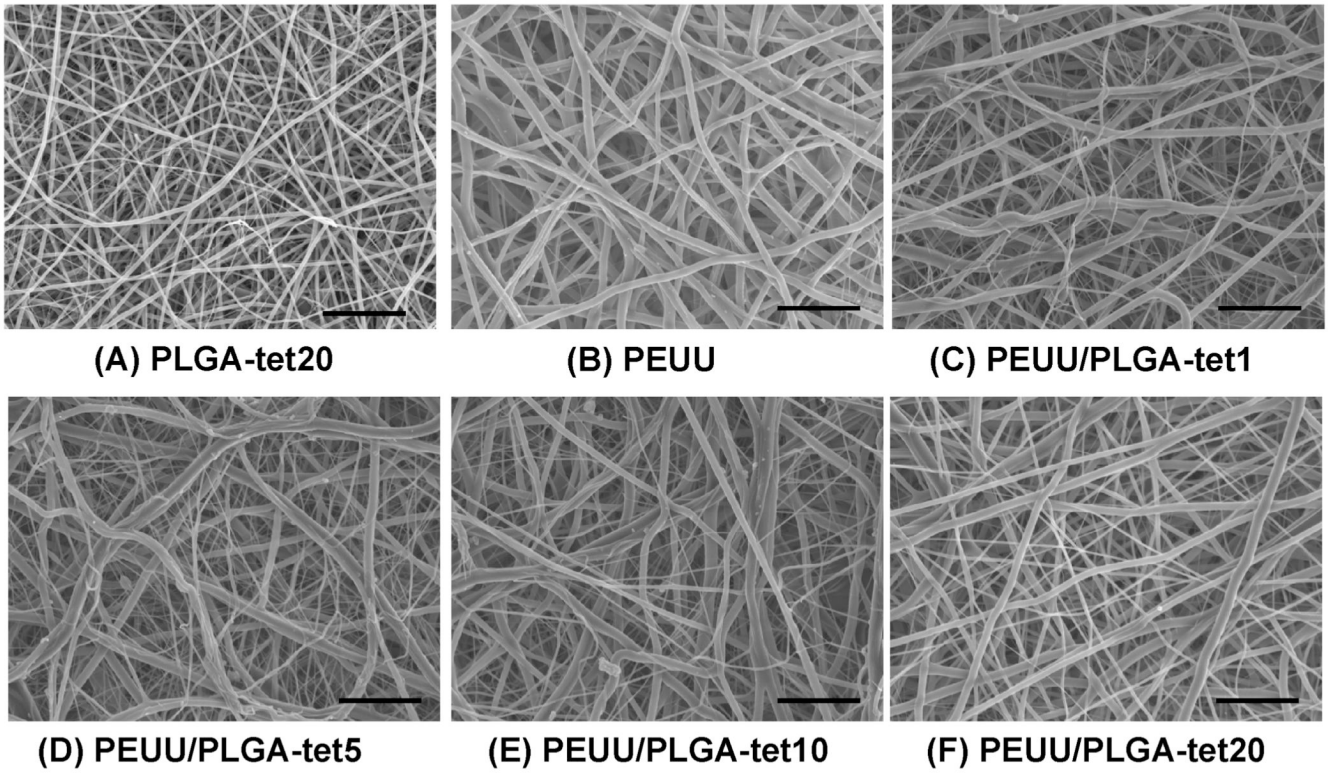

Figure 2.
Scanning electronic micrographs of (A) PLGA-tet20 and (B) PEUU sheets, both fabricated by single-stream electrospinning, and PEUU/PLGA-tet sheets fabricated by two-stream electrospinning with (C) 1, (D) 5, (E) 10 and (F) 20 wt % tet with respect to PLGA. Scale bars = 5 μm.

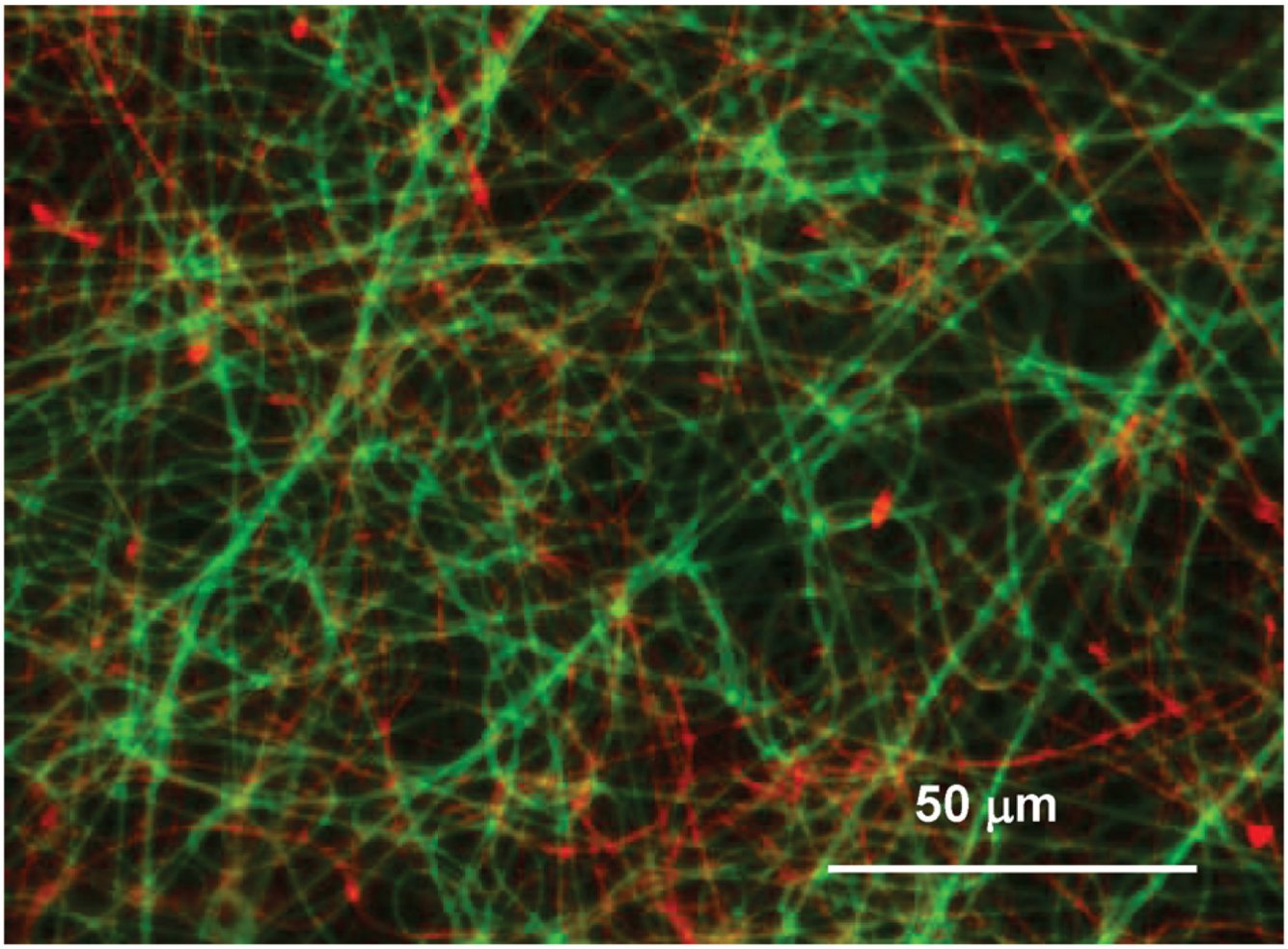

Figure 3.
Fluorescence micrograph of a composite PEUU-FITC/PLGA sheet. Green fibers are PEUU-FITC and red fibers are PLGA.

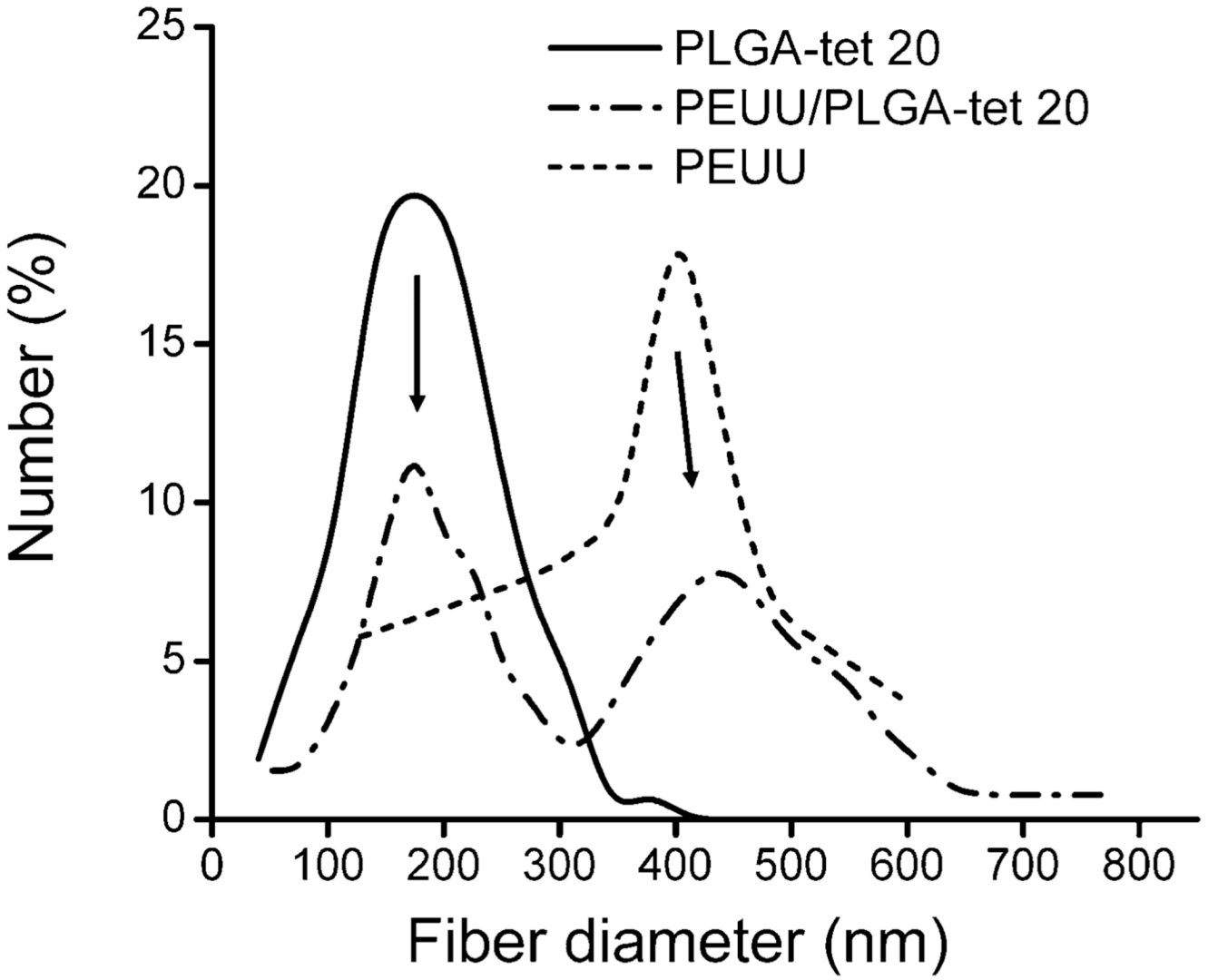

Figure 4.
Fiber diameter distributions of fibrous PLGA-tet20, PEUU, and PEUU/PLGA-tet20 sheets. Arrows indicate the correspondence in fiber diameters between single and double composition sheets.

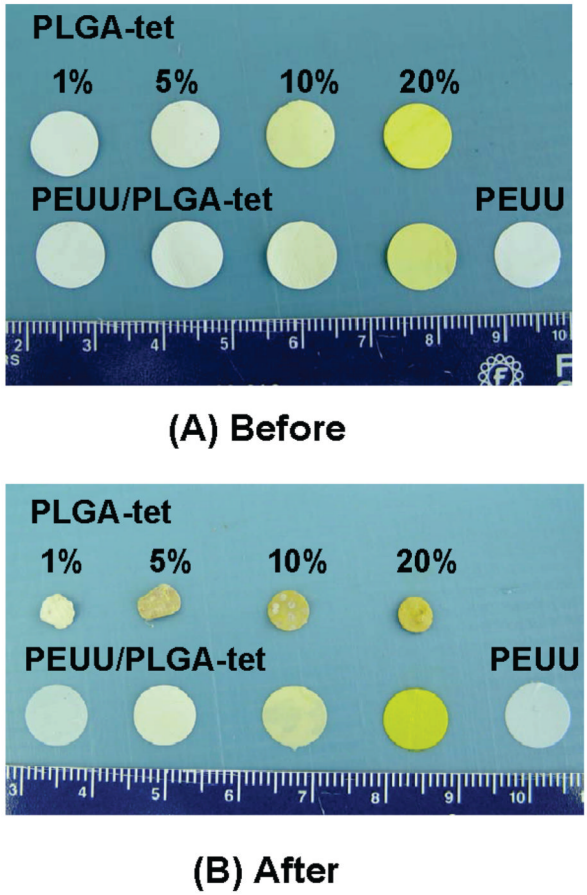

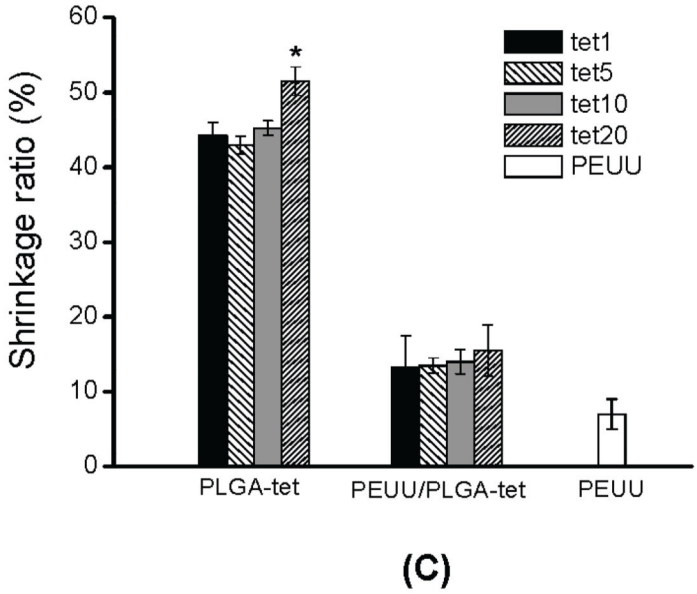

Figure 5.
PLGA-tet, PEUU, and PEUU/PLGA-tet sheets (A) before and (B) after 24 h of immersion in PBS at 37 °C. Scale in cm. (C) The shrinkage ratios of the three sheet types:*, $p < 0.05$ vs other PLGA-tet sheets.

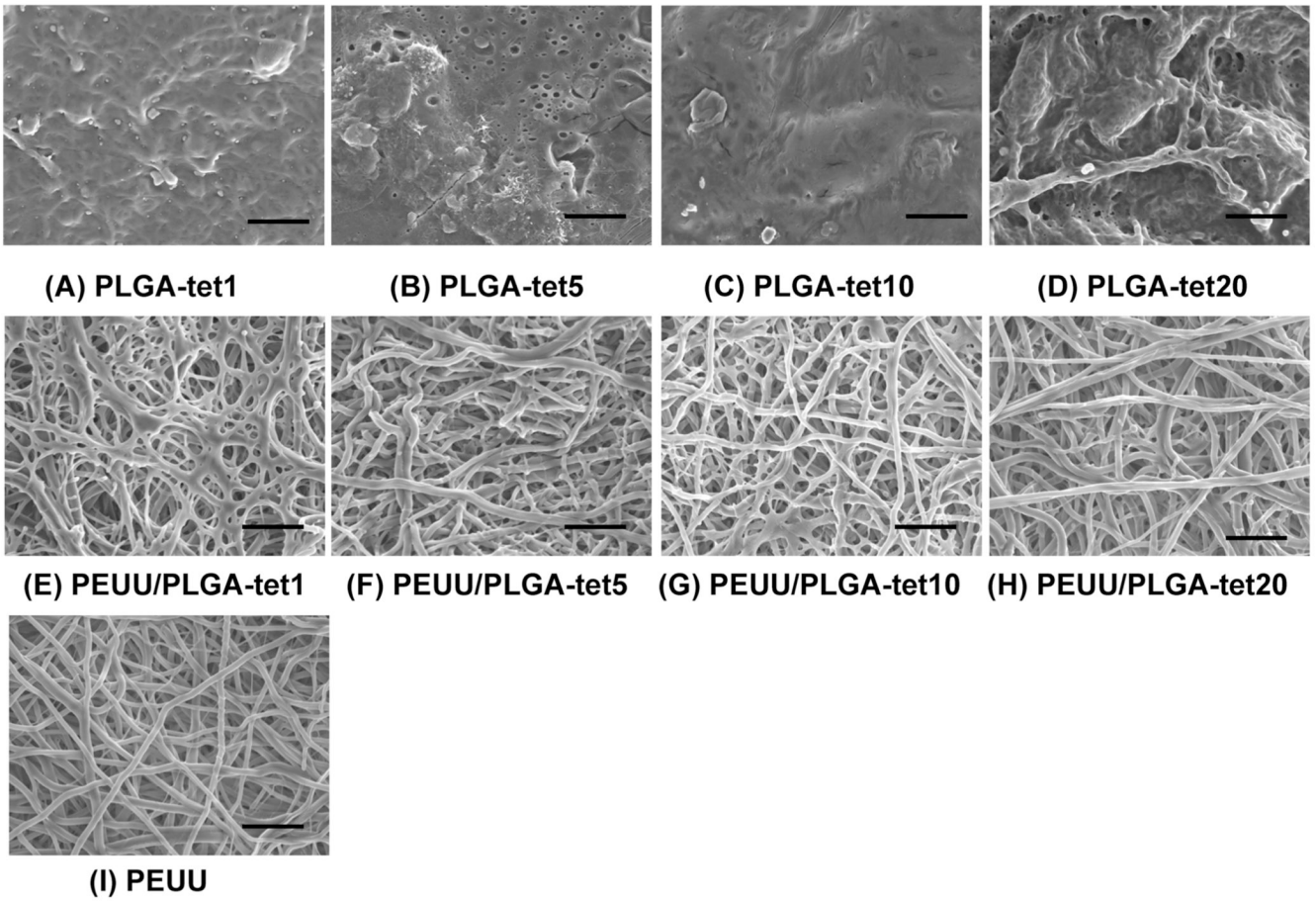

Figure 6.
Scanning electron micrographs of PLGA-tet, PEUU/PLGA-tet, and PEUU sheets after 24 h of immersion in PBS at 37 °C. Scale bars = 5 μm.

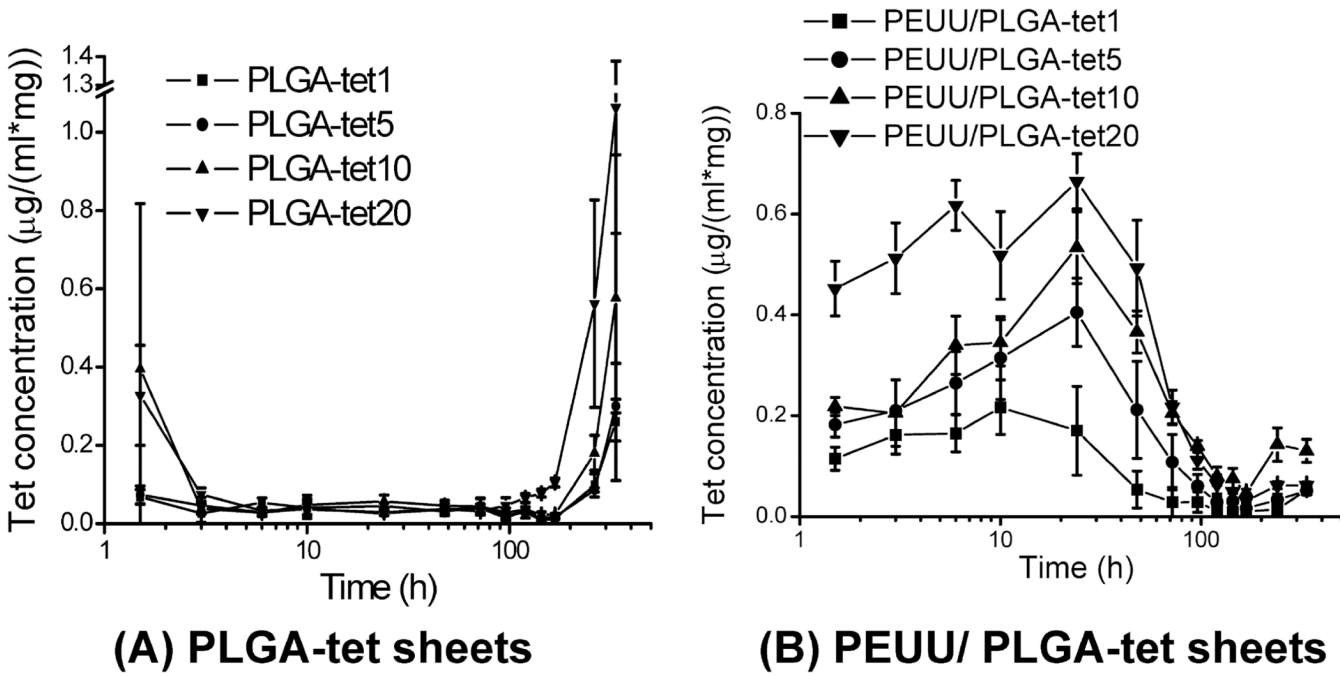

Figure 7.
tet concentration release profiles for (A) PLGA-tet and (B) PEUU/PLGA-tet sheets at each time point after 0.5 h burst release.

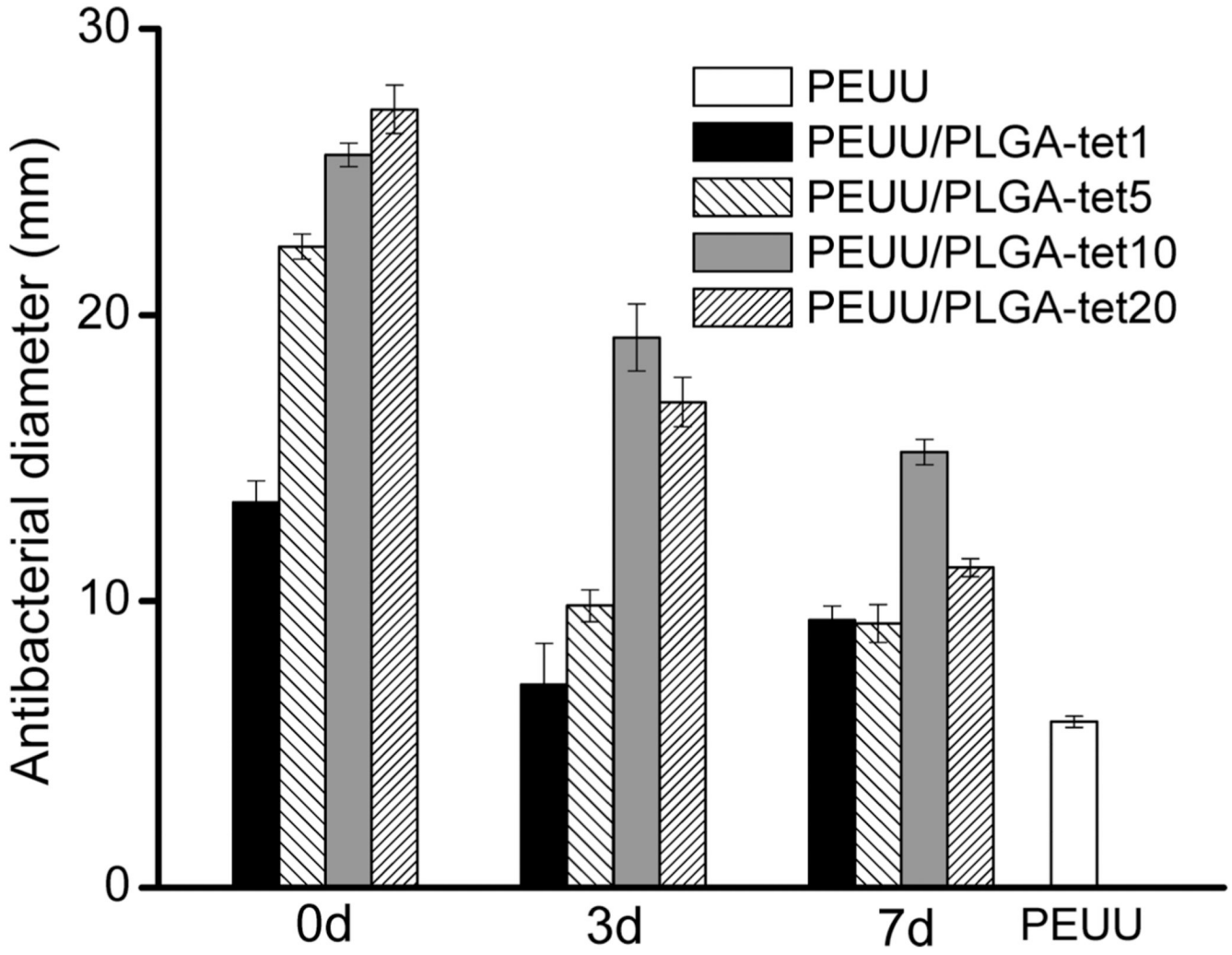

Figure 8.
Antibacterial activity diameters for PEUU/PLGA-tet sheets before (0 days) and after 3 and 7 days of incubation in PBS at 37 °C. The PEUU sheet was used for control purposes.

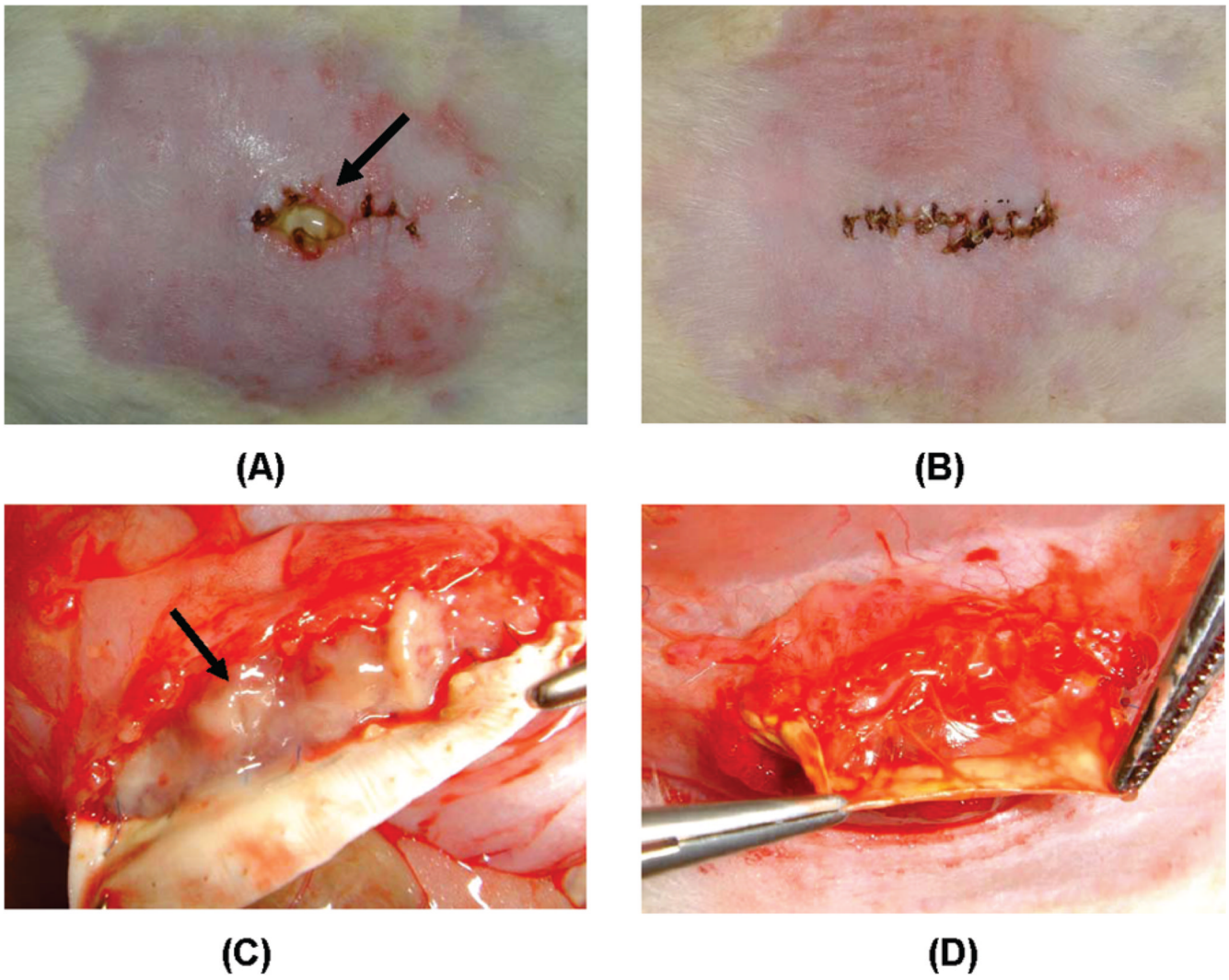

Figure 9.
PEUU and PEUU/PLGA-tet20 sheet implantation sites 1 week after surgical placement with fecal contamination in the rat abdominal wall: (A) wound dehiscence and pus (arrow) on the suture line above the implanted PEUU sheet; (B) no dehiscence associated with the line above the PEUU/PLGA-tet20 sheet; (C) abscess formation (arrow) beneath the lifted PEUU sheet; (D) a lack of abscess formation beneath the PEUU/PLGA-tet20 sheet.

Table 1

PEUU and tet Content in Composite Sheets

sample	PEUU fiber content (wt %)[a]	tet content in composite (wt %)
PEUU/PLGA-tet1	57 ± 2 (70)	0.43 ± 0.02
PEUU/PLGA-tet5	69 ± 2 (70)	1.6 ± 0.1
PEUU/PLGA-tet10	66 ± 1 (68)	3.4 ± 0.1
PEUU/PLGA-tet20	61 ± 1 (66)	7.7 ± 0.2

[a] Values in parentheses are theoretical PEUU content.

Table 2

Mechanical properties

sample	initial modulus (MPa)	100% modulus (MPa)	tensile strength (MPa)	breaking strain (%)	instant strain recovery (%)[a]	suture retention strength (N/mm^2)[b]
PLGA-tet1	55 ± 10		6 ± 1	61 ± 13		
PLGA-tet5	44 ± 4		5 ± 1	30 ± 7		
PLGA-tet10	33 ± 4		4 ± 1	26 ± 7		
PLGA-tet20	14 ± 3		3 ±1	21 ± 4		
PEUU/PLGA-tet1	11 ± 4	4 ± 1	6 ± 1	196 ± 37	94 ± 1	44 ± 5
PEUU/PLGA-tet5	9 ± 4	4 ± 1	7 ± 1	212 ± 32	88 ± 1	36 ± 2
PEUU/PLGA-tet10	8 ± 4	4 ± 1	6 ± 1	182 ± 19	86 ± 4	36 ± 5
PEUU/PLGA-tet20	8 ± 1	3 ± 1	5 ± 1	282 ± 27	87 ± 3	30 ± 2
PEUU	6 ± 1	6 ± 1	12 ± 1	191 ± 15	99 ± 1	71 ± 17

[a] Instant strain recovery was tested at 50% elongation with 1 min hold.

[b] Gore-Tex vascular graft strip, as a control, had a suture retention strength of 23 ± 4 N/mm^2.

Table 3

In Vivo Performance in Abdominal Wall

	PEUU	PEUU/PLGA-tet20
skin dehiscence[a]	23%	2%
abscess formation[b] (above material)	+/++	−
abscess formation[b] (beneath material)	++/+++	−

[a] Skin dehiscence = (length of incision with dehiscence/incision length) × 100%.

[b] Abscess formation qualitatively scored as: − (no abscess visible), + (mild), ++ (moderate), +++ (severe).